2023 62nd IEEE Conference on Decision and Control (CDC)
December 13-15, 2023. Marina Bay Sands, Singapore

Deep Adaptive Indirect Herding of Multiple Target Agents with Unknown Interaction Dynamics

Cristian F. Nino, Omkar Sudhir Patil, Jhyv N. Philor, Zachary I. Bell, and Warren E. Dixon

***Abstract*—The herding problem has received growing interest in the robotics and controls community in recent years. In particular, indirect herding is an abstraction for many potential applications in fields such as wildlife management, crowd control, traffic management, and environment cleanups. Existing works in indirect herding, however, have not taken advantage of recent advances in the field of adaptive control, which have allowed for the development of adaptive controllers using Lyapunov-based deep neural networks (Lb-DNNs). These results, however, are only applicable for systems that are directly controlled, and not for indirect control problems such as the herding problem. This paper develops a novel approach to address the indirect herding problem using an Lb-DNN adaptive backstepping design. The Lb-DNN adaptive backstepping controller enables the herding agent to learn the interaction dynamics and adaptively herd the target agents in real-time, using actual interactions during task-execution. A Lyapunov-based switched systems analysis is used to develop sufficient dwell-time conditions which guarantee exponential convergence of all states to an ultimate bound. Simulations are provided to demonstrate the performance of the developed Lb-DNN adaptive backstepping controller.**

I. Introduction

Animal behaviors have long served as a source of inspiration for technology development. Sheep herding is one such behavior that has garnered attention, wherein a single dog can use its innate herding instincts to coalesce a herd of sheep towards a desired destination. In a broader sense, herding can be defined as the act of having one or more agents drive target agents towards one or more designated locations.

The ability for one (or a small number) of agents to influence the motion of groups of uncontrolled agents in a coordinated manner has implications in a variety of fields. One such application is in high risk manned helicopter operations, particularly those of wildlife management, where the non-cooperative nature of indirect herding can be leveraged to control the movement of wild animals. Developing stable control algorithms for autonomous agents could potentially replace the need for human pilots and reduce fatal accidents [1]. Crowd control is another area where herding behaviors can be applied to great effect. In emergency situations, being able to control the flow of pedestrians is of critical importance. Indirect herding algorithms can be used to direct large groups of people towards safety, preventing overcrowding and potentially hazardous situations. Indirect herding is also applicable for decentralized traffic management of mixed autonomous and human-driven vehicles [2]. Herding behaviors can also be applied in environmental cleanups, such as the collection of oil spills from oil tankers. By building robots that can work cooperatively to collect spilled oil, we can minimize the environmental impact of such incidents [3].

Although existing results provide frameworks for the robot herding problem, continued development is required for more complex herd interactions. For example, results such as [4]–[6] require multiple herder agents, yet a single sheepdog can effectively herd flocks of 80 or more sheep [7]. Moreover, previous works on the herding problem have largely assumed linear, homogeneous, and known interaction dynamics between the herder and target agents [4], [8]; hence, further development is motivated to examine more complex interactions that include nonlinearities, uncertainty, and heterogeneity. Results such as [4], [9], [10] assume the target agents are cohesive and aligned (i.e., flocking behavior). It is not clear how such results could be applied in applications where agents have a fleeing or dispersive behavior.

The result in [11] was the first to consider single agent indirect herding of multiple targets with unknown dynamics. In [11], the herding problem was addressed using a backstepping-based control design, where a single-layer neural network (NN) is used to approximate the unknown herder-target interaction dynamics. However, the NN in [11] only compensates for the uncertainty in the backstepping error dynamics and not the herding error dynamics, i.e., the NN is not used to plan the herder's desired trajectory which acts as the virtual control in the backstepping design. As a result, the herder does not learn how to herd the target agents, which is one of the contributions of the development in this paper.

Recent advances in the field of adaptive control enable the development of adaptive controllers using deep neural networks (DNNs) [12]. While single hidden-layer neural networks are capable of approximating nonlinear functions, DNNs have shown superior performance [13]–[15]. In particular, [12] provides a constructive method to derive control and adaptive update laws for inner and outer layer weights of a Lyapunov-based DNN (Lb-DNN). However,

Cristian F. Nino, Omkar Sudhir Patil, Jhyv N. Philor, and Warren E. Dixon are with the Department of Mechanical and Aerospace Engineering, University of Florida, Gainesville, FL, 32611, USA. Email:{cristian1928, patilomkarsudhir, jhyvphilor, wdixon}@ufl.edu.

Zachary I. Bell is with the Munitions Directorate, Air Force Research Laboratory, Eglin AFB, FL 32542 USA Email: zachary.bell.10@us.af.mil.

This research is supported in part by AFOSR grant FA9550-19-1-0169, AFRL grant FA8651-21-F-1027, and Office of Naval Research grant N00014-21-1-2481. Any opinions, findings and conclusions or recommendations expressed in this material are those of the author(s) and do not necessarily reflect the views of the sponsoring agency.

the result in [12] is only applicable for systems that are directly controlled, unlike indirect control problems such as the herding problem. Specifically, developing Lb-DNN adaptive backstepping controllers is an open problem. Developing adaptive backstepping controllers using Lb-DNNs is challenging because the time-derivative of the Lb-DNN appears in the backstepping error dynamics, which is difficult to address in the ensuing Lyapunov-based stability analysis.

In this paper, we develop a more general control strategy for the herding problem that includes a new Lb-DNN adaptive backstepping design. The design involves two separate Lb-DNNs: one Lb-DNN is used to adaptively plan the herder's desired trajectory as a virtual control, and the other Lb-DNN is used to compensate for the uncertainty in the resulting backstepping error dynamics. We develop new adaptation laws that address the challenges resulting from the time-derivative of the Lb-DNN term in the Lyapunov-based stability analysis. A Lyapunov-based switched systems analysis is used to guarantee that all targets are exponentially regulated to a neighborhood of the goal location. A simulation is presented which shows a herder agent successfully herd 10 target agents to goal locations known only by the herder, in 10.7 seconds.

II. Problem Formulation

Consider a network with one herding agent and a set of $N \in \mathbb{Z}_{>0}$ target agents, denoted by the set $\mathcal{T} \triangleq \{1, 2, \ldots, N\}$. The herding agent's goal is to regulate the positions of the target agents to their respective goal locations. Since there is only one herding agent, we formulate the problem such that the herding agent only chases one target at a time.

The herding agent, whose state is denoted by $y \in \mathbb{R}^n$, must regulate the target agents' states $x_i \in \mathbb{R}^n$, $\forall i \in \mathcal{T}$, to their respective goal locations that are only known by the herding agent. The herding agent's dynamics are modeled as a single integrator, given by

$$\dot{y} = u, \tag{1}$$

where $u \in \mathbb{R}^n$ represents a control input.[1] The target agents are subject to an unknown interaction force that is a function of the distance between the target and the herder. The dynamics for target agent $i \in \mathcal{T}$ is given by

$$\dot{x}_i = g_i(x_i, y)(x_i - y) + h_i(x_i), \tag{2}$$

where $g_i : \mathbb{R}^n \to \mathbb{R}$ is an unknown locally Lipschitz function that defines the interaction dynamics between the i^{th} target agent and the herding agent. The interaction dynamics are assumed to be bounded by $\underline{g_i} \leq g_i(x_i, y) \leq \overline{g_i}$, where $\underline{g_i}, \overline{g_i} \in \mathbb{R}_{>0}$ are known constants. Additionally, $h_i : \mathbb{R}^n \to \mathbb{R}^n$ is an unknown locally Lipschitz function that defines the i^{th} target agent dynamics and is bounded by $\|h_i(x_i)\| \leq \overline{h_i}$, where $\overline{h_i} \in \mathbb{R}_{>0}$ is a known constant. The control objective is to enable the herder to regulate all target agents to their goal locations, given by $x_{i,g} \in \mathbb{R}^n$, despite the target agents' uncertain dynamics and non-cooperative behavior given in (2). The target regulation error is defined as

$$e_i \triangleq x_i - x_{i,g}, \tag{3}$$

where $e_i \in \mathbb{R}^n$.

To herd multiple target agents, a switching strategy must be developed, so that the herding agent chases each target agent, one by one, to its desired goal location. To ensure the closed-loop stability of the switched system, a dwell-time condition must be developed for the switching strategy. We define the set of the currently pursued target agent as $\mathcal{P} \triangleq \{i\}$ and the set of unpursued target agents as $\mathcal{U} \triangleq \mathcal{T} \backslash \mathcal{P}$, where i is an element of $\mathcal{T}$. We use the subscript p when $i \in \mathcal{P}$ the subscript u when $i \in \mathcal{U}$. For notational ease, we omit the index i in the subsequent development. At any given time, a target will either be operating in a pursued or unpursued mode. We use $t_k^p \in \mathbb{R}_{\geq 0}$ and $t_k^u \in \mathbb{R}_{\geq 0}$ to denote the k^{th} instance when target agent $i \in \mathcal{T}$ is switched to the pursued or unpursued mode, respectively, where $k \in \mathbb{N}$.

III. Control Development

Since the target agent dynamics in (2) do not explicitly contain a control input, a backstepping-based control strategy is developed to herd the pursued target agent, where the herder's state y is used as a virtual control input. To facilitate the backstepping strategy, we introduce the backstepping error $\eta_p \in \mathbb{R}^n$ defined as

$$\eta_p \triangleq y_d - y, \tag{4}$$

where $y_d \in \mathbb{R}^n$ denotes the herder's desired trajectory. The target agent dynamics in (2) and the backstepping error in (4) are used to express the time-derivative of the target regulation error in (3) as

$$\dot{e}_p = g_p(x, y)(x + \eta_p - y_d) + h_p(x). \tag{5}$$

Since the interaction dynamics may involve unstructured nonlinear behaviors, we employ Lb-DNNs to adaptively approximate the interaction dynamics in our control strategy. To facilitate the adaptive backstepping strategy, we use two Lb-DNNs in the following section, where one Lb-DNN is used to adaptively plan y_d and the other Lb-DNN is used to adaptively regulate the backstepping error η_p.

A. Deep Neural Network Function Approximation

Let $\Phi_p : \mathbb{R}^{2n \times \sum_{j=0}^{k_p} L_j^p L_{j+1}^p} \to \mathbb{R}^{L_{k_p+1}^p}$ and $\Phi_\eta : \mathbb{R}^{n \times \sum_{j=0}^{k_\eta} L_j^\eta L_{j+1}^\eta} \to \mathbb{R}^{L_{k_\eta+1}^\eta}$ denote the fully connected Lb-DNNs of agent $i \in \mathcal{P}$, defined as $\Phi_p(\kappa, \Theta_p) \triangleq \left(V_{k_p}^{p\top} \phi_{k_p}^p \circ \cdots \circ V_1^{p\top} \phi_1^p\right)(V_0^{p\top} \kappa)$ and $\Phi_\eta(x, \Theta_\eta) \triangleq \left(V_{k_\eta}^{\eta\top} \phi_{k_\eta}^\eta \circ \cdots \circ V_1^{\eta\top} \phi_1^\eta\right)(V_0^{\eta\top} x)$, respectively, where $\kappa \triangleq \left[x^\top, y^\top\right]^\top$, $\Theta_p \triangleq \left[\begin{array}{ccc} \text{vec}\,(V_0^p)^\top & \ldots & \text{vec}\left(V_{k_p}^p\right)^\top \end{array}\right]^\top \in \mathbb{R}^{\sum_{j=0}^{k_p} L_j^p L_{j+1}^p}$, and $\Theta_\eta \triangleq \left[\begin{array}{ccc} \text{vec}\,(V_0^\eta)^\top & \ldots & \text{vec}\left(V_{k_\eta}^\eta\right)^\top \end{array}\right]^\top \in$

[1] Uncertain nonlinear herder dynamics could also be considered using known adaptive control methods for matched uncertainty; however, due to space limitations and the desire to focus the paper on the novel contributions, the dynamics in (1) are considered.

$\mathbb{R}^{\sum_{j=0}^{k_\eta} L_j^\eta L_{j+1}^\eta}$.[2] Additionally, Φ_p has $k_p \in \mathbb{Z}_{\geq 0}$ hidden layers and weight matrices $V_j^p \in \mathbb{R}^{L_j^p \times L_{j+1}^p}$ for all $j \in \{0, \ldots, k_p\}$ with $L_0^p \triangleq 2n$ and $L_{k_p+1}^p \triangleq n$. Similarly, Φ_η has $k_\eta \in \mathbb{Z}_{\geq 0}$ hidden layers and weight matrices $V_j^\eta \in \mathbb{R}^{L_j^\eta \times L_{j+1}^\eta}$ for all $j \in \{0, \ldots, k_\eta\}$, with $L_0^\eta \triangleq n$ and $L_{k_\eta+1}^\eta \triangleq n$, where $L_j^p, L_j^\eta \in \mathbb{Z}_{>0}$ denote the number of neurons in the j^{th} layer of each Lb-DNN, respectively. The smooth activation functions used in Φ_p and Φ_η are denoted by $\phi_j^p : \mathbb{R}^{L_j^p} \to \mathbb{R}^{L_j^p}$ and $\phi_j^\eta : \mathbb{R}^{L_j^\eta} \to \mathbb{R}^{L_j^\eta}$, respectively.

We define $\mathbb{C}(\Omega)$ as the space of continuous functions over the set Ω. The universal function approximation theorem given in [15, Theorem 3.2] states that the function space of DNNs is dense in $\mathbb{C}(\Omega)$. According to the subsequent analysis, κ is guaranteed to remain in a compact set if initialized within some subsequently defined subset of Ω. Hence, for any h_p in $\mathbb{C}(\Omega)$ and a prescribed $\bar{\epsilon}_\eta \in \mathbb{R}_{>0}$, there exist constants $L_j^\eta \in \mathbb{Z}_{>0}$ and an ideal weight vector $\Theta_\eta^* = \left[\operatorname{vec}\left(V_0^{\eta^*}\right)^\top \ \ldots \ \operatorname{vec}\left(V_{k_\eta}^{\eta^*}\right)^\top \right]^\top \in \mathbb{R}^{\sum_{j=0}^{k_\eta} L_j^\eta L_{j+1}^\eta}$ such that $\sup_{x \in \Omega} \| \frac{h_p(x)}{\underline{g_p}} - \Phi_\eta(x, \Theta_p^*) \| \leq \bar{\epsilon}_\eta$. Hence,

$$\Phi_\eta(x, \Theta_\eta^*) + \epsilon_\eta(x) = \frac{h_p(x)}{\underline{g_p}}, \tag{6}$$

where $\epsilon_\eta : \mathbb{R}^n \to \mathbb{R}^{L_{k_\eta+1}^\eta}$ denotes the unknown bounded function approximation error, and $\underline{g_p}$ denotes the known lower bound of $g_p(x, y)$ for target agent $i \in \mathcal{P}$. Similarly, for any g_p and h_p in $\mathbb{C}(\Omega)$ and a prescribed $\bar{\epsilon}_p \in \mathbb{R}_{>0}$, there exist constants $L_j^p \in \mathbb{Z}_{>0}$ and an ideal weight vector $\Theta_p^* = \left[\operatorname{vec}\left(V_0^{p^*}\right)^\top \ \ldots \ \operatorname{vec}\left(V_{k_p}^{p^*}\right)^\top \right]^\top \in \mathbb{R}^{\sum_{j=0}^{k_p} L_j^p L_{j+1}^p}$ such that $\sup_{\kappa \in \Omega} \| g_p(x, y)(x - y) + h_p(x) - \Phi_p(\kappa, \Theta_p^*) \| \leq \bar{\epsilon}_p$. Thus, the unknown interaction and target agent dynamics in (2) can be approximated by an Lb-DNN as

$$\Phi_p(\kappa, \Theta_p^*) + \epsilon_p(\kappa) = g_p(x, y)(x - y) + h_p(x), \tag{7}$$

where $\epsilon_p : \mathbb{R}^n \to \mathbb{R}^{L_{k_p+1}}$ denotes the unknown bounded function approximation error. The function approximation errors are bounded such that $\sup_{\kappa \in \Omega} \|\epsilon_p(\kappa)\| \leq \bar{\epsilon}_p$ and $\sup_{x \in \Omega} \|\epsilon_\eta(x)\| \leq \bar{\epsilon}_\eta$.

Motivated by the subsequent analysis, the weight estimation errors $\widetilde{\Theta}_p \in \mathbb{R}^{\sum_{j=0}^{k_p} L_j^p L_{j+1}^p}$ and $\widetilde{\Theta}_\eta \in \mathbb{R}^{\sum_{j=0}^{k_\eta} L_j^\eta L_{j+1}^\eta}$ are defined as

$$\widetilde{\Theta}_p \triangleq \Theta_p^* - \widehat{\Theta}_p, \tag{8}$$

and

$$\widetilde{\Theta}_\eta \triangleq \Theta_\eta^* - \widehat{\Theta}_\eta, \tag{9}$$

respectively, where $\widehat{\Theta}_p \in \mathbb{R}^{\sum_{j=0}^{k_p} L_j^p L_{j+1}^p}$ and $\widehat{\Theta}_\eta \in \mathbb{R}^{\sum_{j=0}^{k_\eta} L_j^\eta L_{j+1}^\eta}$ are estimates of the Lb-DNN weights. For notational brevity, we introduce the shorthand notations $\Phi_p^* \triangleq \Phi_p(\kappa, \Theta_p^*)$, $\Phi_\eta^* \triangleq \Phi_\eta(x, \Theta_\eta^*)$, $\hat{\Phi}_p \triangleq \Phi_p\left(\kappa, \widehat{\Theta}_p\right)$, and $\hat{\Phi}_\eta \triangleq \Phi_\eta\left(x, \widehat{\Theta}_\eta\right)$.

To facilitate the subsequent development, we make the following assumption [16, Assumption 1]:

Assumption 1. There exist known constants $\overline{\Theta}_\eta \in \mathbb{R}_{>0}$ and $\overline{\Theta}_p \in \mathbb{R}_{>0}$ such that the unknown ideal Lb-DNN weights in (6) and (7) can be bounded as $\|\Theta_\eta^*\| \leq \overline{\Theta}_\eta$ and $\|\Theta_p^*\| \leq \overline{\Theta}_p$, respectively.

B. Control and Adaptation Laws

The herder's desired trajectory is motivated by the desire to minimize the mismatch between a target agent and its goal location. Based on the subsequent stability analysis and the uncertainty in the pursued agent's dynamics, an Lb-DNN is included in the herder's desired trajectory as

$$y_d \triangleq K_p e_p + x_{p,g} + \hat{\Phi}_\eta, \tag{10}$$

where $K_p \in \mathbb{R}_{>0}$ is a user-defined gain. Let $\tilde{g} = g_p(x, y) - \underline{g}$ and note that $0 \leq \tilde{g} \leq \overline{g} - \underline{g}$. By using (3), (6), (10) and the fact that $g_p = \underline{g} + \tilde{g}$, we can rewrite (5) as

$$\begin{aligned} \dot{e}_p(t) = {} & g_p(x, y)(1 - K_p) e_p + g_p(x, y)\eta_p \\ & + \underline{g}\left(\Phi_\eta + \epsilon_\eta(x) - \hat{\Phi}_\eta\right) - \tilde{g}\hat{\Phi}_\eta. \end{aligned} \tag{11}$$

Based on the development in (6), an error model for the Lb-DNN in (6) can be derived using the first-order Taylor series approximation is given by

$$\Phi_\eta^* = \hat{\Phi}_\eta + \hat{\Phi}_\eta' \widetilde{\Theta}_\eta + O\left(\|\widetilde{\Theta}_\eta\|^2\right), \tag{12}$$

where $O\left(\|\widetilde{\Theta}_\eta\|^2\right)$ denotes the higher-order terms, and $\hat{\Phi}_\eta' \triangleq \frac{\partial}{\partial \widehat{\Theta}_\eta} \Phi_\eta(x, \widehat{\Theta}_\eta) \in \mathbb{R}^{L_{k_\eta+1}^\eta \times \sum_{j=0}^{k_\eta} L_j^\eta L_{j+1}^\eta}$. We also define $\Xi_\eta \triangleq \frac{\partial}{\partial x} \Phi_\eta\left(x, \widehat{\Theta}_\eta\right) \in \mathbb{R}^{n \times n}$.

After substituting (12) into (11), we obtain the closed-loop target regulation error dynamics as

$$\begin{aligned} \dot{e}_p(t) = {} & g_p(x, y)(1 - K_p) e_p + g_p(x, y)\eta_p - \tilde{g}\hat{\Phi}_\eta \\ & + \underline{g}\hat{\Phi}_\eta' \widetilde{\Theta}_\eta + \underline{g}\left(O\left(\|\widetilde{\Theta}_\eta\|^2\right) + \epsilon_\eta(x)\right). \end{aligned} \tag{13}$$

The backstepping error dynamics are determined by taking the time-derivative of (4), and using (1), (2), and (7), which yields

$$\dot{\eta}_p = K_p \dot{e}_p + \dot{\hat{\Phi}}_\eta - u(t), \tag{14}$$

where $\dot{\hat{\Phi}}_\eta$ can be obtained using the chain rule and the definitions of Ξ_η and $\hat{\Phi}_\eta'$ as

$$\dot{\hat{\Phi}}_\eta = \Xi_\eta \dot{x} + \hat{\Phi}_\eta' \dot{\widehat{\Theta}}_\eta. \tag{15}$$

Substituting (15) into (14), and using (2) and (3) yields

$$\begin{aligned} \dot{\eta}_p = {} & \left(K_p I_n + \Xi_\eta\right)\left(g_p(x, y)(x - y) + h_p(x)\right) \\ & + \hat{\Phi}_\eta' \dot{\widehat{\Theta}}_\eta - u(t). \end{aligned} \tag{16}$$

[2] $\operatorname{vec}(\cdot)$ denotes the vectorization operator, i.e. given $A \triangleq [a_{i,j}] \in \mathbb{R}^{n \times m}$, $\operatorname{vec}(A) \triangleq [a_{1,1}, \ldots, a_{1,m}, \ldots, a_{n,1}, \ldots, a_{n,m}]^\top$.

Similar to the development for (12), the error model for the Lb-DNN in (7) can be derived using the first-order Taylor series approximation is given by

$$\Phi_p^* = \hat{\Phi}_p + \hat{\Phi}_p' \widetilde{\Theta}_p + O\left(\|\widetilde{\Theta}_p\|^2\right), \tag{17}$$

where $O\left(\|\widetilde{\Theta}_p\|^2\right)$ denotes the higher-order terms, and $\hat{\Phi}_p' \triangleq \frac{\partial}{\partial \widehat{\Theta}_p} \Phi_p(\kappa, \widehat{\Theta}_p) \in \mathbb{R}^{L_{k_p+1}^p \times \sum_{j=0}^{k_p} L_j^p L_{j+1}^p}$.

Based on the subsequent stability analysis, the adaptation laws for the weight estimates of the pursued agent Lb-DNNs are designed as

$$\dot{\widehat{\Theta}}_p \triangleq \Gamma_p \text{proj}\left(\hat{\Phi}_p'^{\top} \left(K_p I_n + \Xi_\eta\right)^\top \eta_p - \sigma_p \widehat{\Theta}_p\right), \tag{18}$$

and

$$\dot{\widehat{\Theta}}_\eta \triangleq \Gamma_\eta \text{proj}\left(\underline{g} \hat{\Phi}_\eta'^{\top} e_p - \sigma_\eta \widehat{\Theta}_\eta\right), \tag{19}$$

where $\Gamma_p, \sigma_p, \Gamma_\eta, \sigma_\eta \in \mathbb{R}_{>0}$ are user defined gains, and I_n is an $n \times n$ identity matrix[3]. In (18) and (19), proj$(\cdot)$ denotes the projection operator defined in [18, Eq.4]. Also motivated by the subsequent stability analysis, the herding agent controller is designed as

$$u(t) \triangleq K_\eta \eta_p + \left(K_p I_n + \Xi_\eta\right) \hat{\Phi}_p + \hat{\Phi}_\eta' \dot{\widehat{\Theta}}_\eta, \tag{20}$$

where $K_\eta \in \mathbb{R}_{>0}$ is a user-defined gain. Substituting (7), (17), (19), and (20) into (16), yields the backstepping closed-loop error dynamics

$$\dot{\eta}_p = \left(K_p I_n + \Xi_\eta\right)\left(\hat{\Phi}_p' \widetilde{\Theta}_p + O\left(\|\widetilde{\Theta}_p\|^2\right) + \epsilon_p(\kappa)\right) - K_\eta \eta_p. \tag{21}$$

Remark 1. Due to the use of the projection operator, the Lb-DNN weight estimates are bounded. Furthermore, because the input is contained within a compact set, there exists values of $\overline{\Phi}_p \in \mathbb{R}_{>0}$ and $\overline{\Phi}_\eta \in \mathbb{R}_{>0}$ such that $\|\hat{\Phi}_p\| \leq \overline{\Phi}_p$ and $\|\hat{\Phi}_\eta\| \leq \overline{\Phi}_\eta$. Therefore, we can bound $\tilde{g}\hat{\Phi}_\eta$ as $\|\tilde{g}\hat{\Phi}_\eta\| \leq \left(\overline{g} - \underline{g}\right)\overline{\Phi}_p$.

Remark 2. The projection operator in (18) and (19) ensures that $\widehat{\Theta}_p(t) \in \mathcal{B}^p \triangleq \left\{\varsigma \in \mathbb{R}^{\sum_{j=0}^{k_p} L_j^p L_{j+1}^p} : \|\varsigma\| \leq \overline{\Theta}_p\right\}$ and $\widehat{\Theta}_\eta(t) \in \mathcal{B}^\eta \triangleq \left\{\varsigma \in \mathbb{R}^{\sum_{j=0}^{k_\eta} L_j^\eta L_{j+1}^\eta} : \|\varsigma\| \leq \overline{\Theta}_\eta\right\}, \forall t \in \mathbb{R}_{\geq 0}$.

Remark 3. Suppose that $x, y \in \Omega$. Due to the use of the projection operator and Assumption 1, the unknown Lb-DNN weights can be bounded as $\|\widetilde{\Theta}_p\| \leq \|\Theta_p^*\| + \|\widehat{\Theta}_p\| = 2\overline{\Theta}_p$ and $\|\widetilde{\Theta}_\eta\| \leq \|\Theta_\eta^*\| + \|\widehat{\Theta}_\eta\| = 2\overline{\Theta}_\eta$, respectively. Therefore, due to the smoothness of the Lb-DNN and the boundedness of $\widetilde{\Theta}_p$ and $\widetilde{\Theta}_\eta$, there exist known constants $\Delta_p \in \mathbb{R}_{>0}$ and $\Delta_\eta \in \mathbb{R}_{>0}$ such that $\left\|O\left(\|\widetilde{\Theta}_p\|^2\right)\right\| \leq \Delta_p$ and $\left\|O\left(\|\widetilde{\Theta}_\eta\|^2\right)\right\| \leq \Delta_\eta$.

IV. Stability Analysis

This stability analysis considers the behavior of the i^{th} target when it is in the pursued and unpursued modes, and then a combined switched systems analysis is provided to quantify the behavior of the overall state trajectories. Theorem 1 proves that during periods when a target operates in the pursued mode, the system states associated with the pursued target agent exponentially converge to an ultimate bound. When the target agent is operating in the unpursued mode, Theorem 2 shows that the unpursued agent's states remain bounded for all bounded t. Considering these results, the overall trajectories are analyzed in Theorem 3, and a sufficient maximum dwell-time condition is provided which, when satisfied, ensures all agent states remain bounded for all time.

A. Target operating in the pursued mode

Consider an arbitrary target agent $i \in \mathcal{P}$. To facilitate the following analysis, we introduce the auxiliary constants $\delta_1, \delta_2, \varepsilon \in \mathbb{R}_{>0}$ defined as $\delta_1 \triangleq \left(\overline{g} - \underline{g}\right)\overline{\Phi}_p + \underline{g}\left(\Delta_\eta + \bar{\epsilon}_\eta\right)$, $\delta_2 \triangleq \left(\Delta_p + \bar{\epsilon}_p\right)\|K_p I_n + \Xi_\eta\|_F$ and $\varepsilon_p \triangleq 2\sigma_p \overline{\Theta}_p^2 + 2\sigma_\eta \overline{\Theta}_\eta^2 + \frac{\delta_1^2 + \delta_2^2}{2}$. Let $\xi \triangleq \begin{bmatrix} e_p^\top & \eta_p^\top & \widetilde{\Theta}_p^\top & \widetilde{\Theta}_\eta^\top \end{bmatrix}^\top \in \mathbb{R}^\Psi$ denote a concatenated state, where $\Psi \triangleq 2n + \sum_{j=0}^{k_p} L_j^p L_{j+1}^p + \sum_{j=0}^{k_\eta} L_j^\eta L_{j+1}^\eta$ and consider the continuously differentiable Lyapunov function candidate $V_p : \mathbb{R}^\Psi \to \mathbb{R}_{\geq 0}$ defined as

$$V_p(\xi) \triangleq \frac{1}{2} e_p^\top e_p + \frac{1}{2}\eta_p^\top \eta_p + \frac{1}{2}\widetilde{\Theta}_p^\top \Gamma_p^{-1} \widetilde{\Theta}_p + \frac{1}{2}\widetilde{\Theta}_\eta^\top \Gamma_\eta^{-1} \widetilde{\Theta}_\eta. \tag{22}$$

The candidate Lyapunov function in (22) satisfies

$$\alpha_1 \|\xi\|^2 \leq V_p(\xi) \leq \alpha_2 \|\xi\|^2, \tag{23}$$

where $\alpha_1 \triangleq \frac{1}{2}\min\left\{1, \Gamma_p^{-1}, \Gamma_\eta^{-1}\right\}$ and $\alpha_2 \triangleq \frac{1}{2}\max\left\{1, \Gamma_p^{-1}, \Gamma_\eta^{-1}\right\}$. Similarly, we define $\beta, \gamma_p \in \mathbb{R}_{>0}$ as $\beta \triangleq \min\left\{K_p, K_\eta, \sigma_p, \sigma_\eta\right\}$, and $\gamma_p \triangleq \frac{\beta}{\alpha_2}$. Let

$$\mathcal{B}_\Lambda \triangleq \left\{\varsigma \in \mathbb{R}^\Psi : \|\varsigma\| < \omega\sqrt{\frac{\alpha_1}{\alpha_2}}\right\}, \tag{24}$$

$$\mathcal{B}_\Upsilon \triangleq \left\{\varsigma \in \Omega : \|\varsigma\| < (2 + K_p)\omega + 2\|x_{p,g}\| + \overline{\Phi}_p\right\}, \tag{25}$$

denote open and connected sets, where $\omega \in \mathbb{R}_{\geq 0}$ is a prescribed bound on $\|\xi\|$.

Theorem 1. *Consider the dynamical systems described in (1) and (2). For any initial conditions of the states $\xi(t_0)$ in $\mathcal{B}_\Lambda$, the controller in (20) and the adaptation laws in (18) and (19) guarantee that*

$$\|\xi(t)\| \leq \sqrt{\left(\frac{\alpha_2}{\alpha_1}\|\xi(t_0)\|^2 - \frac{\varepsilon_p}{\gamma_p \alpha_1}\right)\mathrm{e}^{-\gamma_p(t-t_0)} + \frac{\varepsilon_p}{\gamma_p \alpha_1}}, \tag{26}$$

$\forall t \in [t_k^p, t_k^u)$, provided that Assumption 1 is satisfied, and the control gains K_p and K_η are selected such that $K_p > \frac{3\overline{g}+1}{2\underline{g}}$ and $K_\eta > \frac{\overline{g}+1}{2}$.

Proof: By using (13), (20), (21), and Remark 1, we can

[3] Ξ_η, $\hat{\Phi}_p'$, and $\hat{\Phi}_\eta'$ may be computed via [17, Eq.(11-13)]

upper bound the time-derivative of V_p as

$$\begin{aligned}\dot{V}_p(\xi) \leq{}& (1-K_p)\overline{g}\|e_p\|^2 + \overline{g}\|e_p\|\|\eta_p\| - K_\eta\|\eta_p\|^2 \\ &+ \left(\left(\overline{g}-\underline{g}\right)\overline{\Phi}_p + \underline{g}\left(\Delta_\eta + \overline{\epsilon}_\eta\right)\right)\|e_p\| \\ &+ \left(\Delta_p + \overline{\epsilon}_p\right)\|K_pI_n + \Xi_\eta\|_F\|\eta_p\| \\ &+ \eta_p^\top\left(K_pI_n + \Xi_\eta\right)\hat{\Phi}_p'\widetilde{\Theta}_p - \widetilde{\Theta}_p^\top\Gamma_p^{-1}\dot{\widehat{\Theta}}_p \\ &+ \underline{g}e_p^\top\hat{\Phi}_\eta\widetilde{\Theta}_\eta - \widetilde{\Theta}_\eta^\top\Gamma_\eta^{-1}\dot{\widehat{\Theta}}_\eta. \end{aligned} \tag{27}$$

Applying Young's inequality to (27) and using the definition of δ_1 and δ_2, we have

$$\begin{aligned}\dot{V}_p(\xi) \leq{}& \left(\frac{3\overline{g}+1}{2} - \overline{g}K_p\right)\|e_p\|^2 + \left(\frac{\overline{g}}{2} - K_\eta + \frac{1}{2}\right)\|\eta_p\|^2 \\ &+ \eta_p^\top\left(K_pI_n + \Xi_\eta\right)\hat{\Phi}_p'\widetilde{\Theta}_p - \widetilde{\Theta}_p^\top\Gamma_p^{-1}\dot{\widehat{\Theta}}_p \\ &+ \underline{g}e_p^\top\hat{\Phi}_\eta\widetilde{\Theta}_\eta - \widetilde{\Theta}_\eta^\top\Gamma_\eta^{-1}\dot{\widehat{\Theta}}_\eta + \frac{\delta_1^2+\delta_2^2}{2}. \end{aligned} \tag{28}$$

Substituting (18) and (19) into (28), applying the gain conditions to K_p and K_η, and using (8) and (9), yields the inequality

$$\begin{aligned}\dot{V}_p(\xi) \leq{}& -K_p\|e_p\|^2 - K_\eta\|\eta_p\|^2 + \sigma_p\widetilde{\Theta}_p^\top\widehat{\Theta}_p \\ &+ \sigma_\eta\widetilde{\Theta}_\eta^\top\widehat{\Theta}_\eta + \frac{\delta_1^2+\delta_2^2}{2}. \end{aligned} \tag{29}$$

Substituting the upper bounds given by Assumption 1 and Remark 1, using the definitions of γ_p, ϵ, and β and applying the upper bound of (23) to the resulting inequality, we can upper bound (29) as

$$\begin{aligned}\dot{V}_p(\xi) &\leq -\beta\|\xi\|^2 + 2\sigma_p\overline{\Theta}_p^2 + 2\sigma_\eta\overline{\Theta}_\eta^2 + \frac{\delta_1^2+\delta_2^2}{2}, \\ &= -\gamma_pV_p(\xi) + \varepsilon_p. \end{aligned} \tag{30}$$

Solving the differential inequality in (30) and using (22), yields (26).

Consider the case where $\xi(0) \in \mathcal{B}_\Lambda$. By (24), we obtain $\|\xi(0)\| \leq \omega\sqrt{\frac{\alpha_1}{\alpha_2}}$. This implies that $\sqrt{\frac{\alpha_2}{\alpha_1}}\|\xi(0)\| \leq \omega$. Using equation (23) and the non-increasing property of V_p, $\|\xi(t)\| \leq \sqrt{\frac{V_p(\xi(t))}{\alpha_1}} \leq \sqrt{\frac{V_p(\xi(0))}{\alpha_1}} \leq \sqrt{\frac{\alpha_2\|\xi(0)\|^2}{\alpha_1}}$. Therefore, $\|\xi(t)\| \leq \omega$ which implies $\|e_p(t)\| \leq \omega$ and $\|\eta_p(t)\| \leq \omega$. Using (3), (4), (10), applying the triangle inequality to the resulting terms, and using Remark 1 yields

$$\begin{aligned}\|\kappa(t)\| &\leq \|e_p + x_{p,g}\| + \|\eta_p + K_pe_p + x_{p,g} + \hat{\Phi}_\eta\|, \\ &\leq (2+K_p)\,\omega + 2\|x_{p,g}\| + \overline{\Phi}_\eta. \end{aligned} \tag{31}$$

Thus, by (25), if $\xi(0) \in \mathcal{B}_\Lambda$, then $\kappa(t) \in \mathcal{B}_\Upsilon$.

Since $e_p, \eta_p, \widetilde{\Theta}_p, \widetilde{\Theta}_\eta \in \mathcal{L}_\infty$, using (3) yields that $x, y_d, y \in \mathcal{L}_\infty$. From Remark 1, we know that $\hat{\Phi}_\eta, \hat{\Phi}_p \in \mathcal{L}_\infty$. Using the projection property, we can conclude that $\widehat{\Theta}_p$ and $\widehat{\Theta}_\eta$ are bounded. Since Φ_p and Φ_η are smooth, their first derivatives Φ_p' and Φ_η' are continuous. Because all inputs to Φ_p' and Φ_η' are bounded, $\Phi_p', \Phi_\eta' \in \mathcal{L}_\infty$. From the above analysis, $\eta_p, \Phi_\eta, \hat{\Phi}_p, e_p$, and $\widehat{\Theta}_\eta$ are all in $\mathcal{L}_\infty$. This implies that $u(t) \in \mathcal{L}_\infty$, and therefore, $\dot{\eta}_p \in \mathcal{L}_\infty$. By the universal function approximation, together with the fact that $\eta_p, \Phi_\eta, \hat{\Phi}_\eta$, and e_p are in $\mathcal{L}_\infty$, we have that $\dot{e}_p \in \mathcal{L}_\infty$. By Remark 2, we can use the projection property again, along with the fact that $\Phi_p', \Phi_\eta', \widehat{\Theta}_p, \widehat{\Theta}_\eta, \Xi_\eta \in \mathcal{L}_\infty$, to show that $\dot{\widehat{\Theta}}_p, \dot{\widehat{\Theta}}_\eta \in \mathcal{L}_\infty$. As a result, we can conclude that all the closed-loop signals are bounded. ∎

B. Target operating in the unpursued mode

Since $\text{card}(\mathcal{U}) \geq 1$, we introduce the subscript u to denote the $i \in \mathcal{U}$ agent(s). Since i is arbitrary, this analysis applies to all target agents in the unpursued mode. To facilitate the following analysis, we introduce the auxiliary constants $\gamma_u, \varepsilon_u \in \mathbb{R}_{>0}$ defined as $\gamma_u \triangleq 2\left(\overline{g}_u + \frac{1}{2}\overline{g}_u\overline{x}_{u,g} + \frac{1}{2}\overline{g}_u\overline{y} + \frac{1}{2}\overline{h}_u\right)$, and $\varepsilon_u \triangleq \frac{1}{2}\overline{g}_u\overline{x}_{u,g} + \frac{1}{2}\overline{g}_u\overline{y} + \frac{1}{2}\overline{h}_u$. Consider the continuously differentiable Lyapunov function candidate $V_u : \mathbb{R}^n \to \mathbb{R}_{\geq 0}$ defined as

$$V_u(e_u) \triangleq \frac{1}{2}e_u^\top e_u. \tag{32}$$

Theorem 2. *During $t \in \left[t_k^u, t_{k+1}^p\right)$ $\forall k \in \mathbb{N}$, the system states associated with target $i \in \mathcal{U}$ remain bounded as*

$$\|e_u(t)\| \leq \sqrt{\left(\|e_u(t_0)\|^2 + \frac{\varepsilon_u}{\gamma_u}\right)\mathrm{e}^{\gamma_u(t-t_0)} - \frac{\varepsilon_u}{\gamma_u}}. \tag{33}$$

Proof: By using the upper bounds of (2), we can upper bound the time-derivative of (32) as

$$\dot{V}_u(t) \leq \overline{g}_u\|e_u\|^2 + \overline{g}_u\|e_u\|\|x_{u,g}\| + \overline{g}_u\|y\|\|e_u\| + \overline{h}_u\|e_u\|. \tag{34}$$

Based on the bound on κ in (31), y is bounded by some $\overline{y} \in \mathbb{R}_{>0}$. Observing that $\|x_{u,g}\|$ is bounded by design, we can upper bound (34) as

$$\dot{V}_u(t) \leq \overline{g}_u\|e_u\|^2 + \overline{g}_u\overline{x}_{u,g}\|e_u\| + \overline{g}_u\overline{y}\|e_u\| + \overline{h}_u\|e_u\|. \tag{35}$$

Applying Young's inequality to (35) and using the definitions of γ_u and ε_u, we have

$$\dot{V}_u(t) \leq \gamma_uV_u(t) + \varepsilon_u. \tag{36}$$

Solving the differential inequality given by (36) yields (33). ∎

C. Combined analysis

Here, we consider $i \in \mathcal{T}$, for all time. Since $\mathcal{T} = \mathcal{U} \cup \mathcal{P}$ and $\mathcal{U}$ and $\mathcal{P}$ are disjoint, the combined analysis considers all possible arrangements of the system. The bound given by (26) is applicable at times $t \in [t_k^p, t_k^u)$. Similarly, the bound given by (33) is applicable at times $t \in \left[t_k^u, t_{k+1}^p\right)$. The combined analysis aims to find a sufficient condition that, if satisfied, will ensure the bounds in (26) and (33) are true for all $t \in \mathbb{R}_{>0}$. Motivated by this aim, we define $\Delta t_k^p, \Delta t_k^u \in \mathbb{R}_{>0}$ as $\Delta t_k^p \triangleq t_k^u - t_k^p$ and $\Delta t_k^u \triangleq t_{k+1}^p - t_k^u$.

Theorem 3. *The controller in (20) and the adaptation laws in (18) and (19) guarantee that the target regulation error(s) associated with target agent(s) $i \in \mathcal{T}$ remain(s) bounded as $\|e_i(t)\| \leq \sqrt{\left(\frac{\alpha_2}{\alpha_1}\|\xi(t_0)\|^2 - \frac{\varepsilon_p}{\gamma_p\alpha_1}\right)\mathrm{e}^{-\gamma_p(t-t_0)} + \frac{\varepsilon_p}{\gamma_p\alpha_1}}$, for all time $t \in \mathbb{R}_{\geq 0}$, provided $\Delta t_k^u < \tau$, where*

$$\tau \leq \frac{1}{\gamma_u}\ln\left[\frac{\frac{\alpha_2}{\alpha_1}\|e_p(t_k^p)\|^2 + \frac{\varepsilon_u}{\gamma_u}}{\|e_u(t_k^u)\|^2 + \frac{\varepsilon_u}{\gamma_u}}\right]. \tag{37}$$

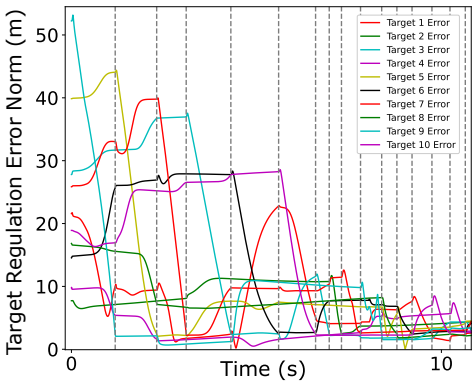

Figure 1. Plots of the normalized target regulation error $\|e_i\|$ for $i \in [1, 10]$ and the instants when the herder switches between targets.

Proof: Based on (26), the stated bound on $\|e_i(t)\|$ holds if $\|e_u(t)\| \leq \|e_p(t)\|$, for all $t \in \mathbb{R}_{\geq 0}$.[4] Since we start in the pursued mode, we have that for $\|e_p(t)\|$, $t_0 = t_k^p$ and $t_f = t_k^u$. Similarly, for $\|e_u(t)\|$ we have that $t_0 = t_k^u$ and $t_f = t_{k+1}^p$. Using $\|e_u(t)\| \leq \|e_p(t)\|$, (26), and (33), taking the natural logarithm of the resulting expression, and using $\exp(-\gamma_p \Delta t_k^p) \leq 1$, we arrive at (37). ∎

V. Simulation

Simulations are performed to evaluate the performance of the developed method. The herding agent is tasked with regulating 10 target agents ($N = 10$) to 10 separate goal locations known only by the herding agent. The dynamics for the agents are given by $g_i(x_i, y) \triangleq a_i \exp\left(\frac{1}{2\mu}(x_i - y)^\top (x_i - y)\right)$ and $h_i(x_i) \triangleq [[b_{i,1}\sin(x_{i,2})], [b_{i,2}\cos(x_{i,1})]]^\top$ [m], where $x_i \triangleq [x_{i,1}, x_{i,2}]^\top$, $a_i \in [5, 15]$, $\mu \in [64, 128]$, and $b_{i,1}, b_{i,2} \in [-1, 1]$.

The planar coordinates for the initial positions of all agents were randomly selected from a uniform distribution $U(-25, 25)$, as were the goal location for the target agents. The subsequent target agent to be herded was determined using the expression $i_{\text{next}} = \arg\max_{i \in \mathcal{T}} \|e_i\|$, which ensures that $\|e_u| < \|e_p\|$. An agent was determined to reach its goal location if it was within a radius of 2.5 meters of the goal coordinate. The simulation concluded when all targets were simultaneously inside their designated goal areas.

The Lb-DNN weight estimates were initialized with random values drawn from a uniform distribution $U(-0.5, 0.5)$. The parameters were selected as $\overline{\Theta}_p, \overline{\Theta}_\eta = 5$, $\Gamma_\eta = 0.01$, $\sigma_\eta = 0.1$, $\Gamma_p = 2.5$, and $\sigma_p = 0.1$. The Lb-DNN's Φ_p and Φ_η were selected with 4 hidden layers and 5 neurons in each layer. The control gains K_p and K_η are selected as $K_p = \frac{3\overline{g}+1}{2\overline{g}} + 0.25$ and $K_\eta = \frac{\overline{g}+1}{2} + 0.001$, where $\overline{g} = 100$.

Figure 1 provides the plot of the target regulation error for each target agent. The dotted lines in the figure indicate the time-instants when the herding switched to a different target agent. As evident from Figure 1, all target agents were effectively herded with $\|e\| < 10$ in about 6 seconds. By 10.7 seconds, the herding agent had successfully brought all target agents within their respective containment zones.

[4]This case can always be guaranteed by the decision logic for when to chase the next target [11, Theorem 1].

VI. Conclusion

This paper develops an approach to address the herding problem by developing an Lb-DNN adaptive backstepping controller. The Lb-DNN adaptive backstepping controller enables the herding agent to learn the interaction dynamics and adaptively herd the target agents in real-time, using actual interactions during task-execution. Simulations are provided to demonstrate the performance of the developed controller, and the Lyapunov-based switched system analyses ensure exponential convergence of all states to an ultimate bound. Future efforts could leverage the new developments in this paper to examine the ensemble herding problem formulated in [4], [5], [11]. These efforts could involve expanding the application of Lb-DNN adaptive backstepping control to a wider array of indirect control challenges, encompassing more complex and higher-dimensional interaction dynamics.

References

[1] W. M. K. Mark Colborn, Scott Burgess, "Helicopter safety enhancement 90 formal report," *Fed. Aviat. Agen.*, 2019.

[2] A. Bazzan and F. Klugl, *Multi-Agent Systems for Traffic and Transportation Engineering*. 2009.

[3] M. Fingas, *The Basics of Oil Spill Cleanup*. CRC Press, 2013.

[4] A. Pierson and M. Schwager, "Controlling noncooperative herds with robotic herders," *IEEE Trans. Robot.*, vol. 34, no. 2, pp. 517–525, 2018.

[5] E. Sebastian and Montijano, "Multi-robot implicit control of herds," in *IEEE Int. Conf. on Robot. and Autom.*, pp. 1601–1607, 2021.

[6] W. Lee and D. Kim, "Autonomous shepherding behaviors of multiple target steering robots," *Sensors*, vol. 17, no. 12, p. 2729, 2017.

[7] L. Coppinger and R. Coppinger, "Dogs for herding and guarding livestock," *CABI Books*, pp. 254–270, 2019.

[8] W. Scott and N. E. Leonard, "Pursuit, herding and evasion: A three-agent model of caribou predation," in *Proc. IEEE Amer. Cont. Conf.*, pp. 2978–2983, June 2013.

[9] C. W. Reynolds, "Flocks, herds and schools: A distributed behavioral model," in *Proc. of the 14th Annual Conf. on Comp. Graph. and Inter. Techn.* (M. C. Stone, ed.), pp. 25–34, ACM, 1987.

[10] T. Miki and T. Nakamura, "An effective simple shepherding algorithm suitable for implementation to a multi-mobile robot system," in *Proc. of the First Int. Conf. on Innov. Computing, Inf., and Control*, vol. 3, (Washington, DC, USA), pp. 161–165, 2006.

[11] R. Licitra, Z. Bell, and W. Dixon, "Single agent indirect herding of multiple targets with unknown dynamics," *IEEE Trans. Robotics*, vol. 35, no. 4, pp. 847–860, 2019.

[12] O. Patil, D. Le, M. Greene, and W. E. Dixon, "Lyapunov-derived control and adaptive update laws for inner and outer layer weights of a deep neural network," *IEEE Control Syst. Lett.*, vol. 6, pp. 1855–1860, 2022.

[13] Y. LeCun, Y. Bengio, and G. Hinton, "Deep learning," *Nature*, vol. 521, no. 7553, pp. 436–444, 2015.

[14] D. Rolnick and M. Tegmark, "The power of deeper networks for expressing natural functions," in *Proc. Int. Conf. Learn. Represent.*, pp. 1–14, 2018.

[15] P. Kidger and T. Lyons, "Universal approximation with deep narrow networks," in *Conf. Learn. Theory*, pp. 2306–2327, PMLR, 2020.

[16] F. L. Lewis, A. Yegildirek, and K. Liu, "Multilayer neural-net robot controller with guaranteed tracking performance," *IEEE Trans. Neural Netw.*, vol. 7, no. 2, pp. 388–399, 1996.

[17] O. S. Patil, D. M. Le, E. Griffis, and W. E. Dixon, "Deep residual neural network (ResNet)-based adaptive control: A Lyapunov-based approach," in *Proc. IEEE Conf. Decis. Control*, 2022.

[18] Z. Cai, M. S. de Queiroz, and D. M. Dawson, "A sufficiently smooth projection operator," *IEEE Trans. Autom. Control*, vol. 51, pp. 135–139, Jan. 2006.